

ZONALLY LOCALIZED STORM TRACKS IN AN IDEALIZED AGCM

¹Masaru Inatsu*, ¹Hitoshi Mukougawa, and ²Shang-Ping Xie¹Hokkaido University, Sapporo, Japan; ²University of Hawaii/IPRC, Honolulu, HI

1. INTRODUCTION

In the Northern Hemisphere winter, storm tracks characterized by high activity of synoptic-scale disturbances are zonally localized downstream of the westerly jet cores in both the Pacific and Atlantic sectors (Blackmon, 1977). Hoskins and Valdes (1990) shows that high baroclinicity regions near the surface exist just upstream of the storm tracks. It is suggested that the baroclinic energy conversion from the time-mean flow to eddies is dominant at the developing stage of transient eddies, while the ageostrophic energy transfer is essential for the downstream development of storm tracks (*e.g.* Chang and Orlanski, 1993). Therefore, without the dissipation mechanism, the storm track extends into further downstream and may not be localized in the zonal direction. The most promising candidate to dissipate transient eddies is the barotropic energy conversion from eddies to the time-mean diffusive regions (Whitaker and Dole, 1995). On the other hand, Shutts (1983) denoted an important role of the low-frequency variability on dissipating synoptic-scale eddies. However, these proposed mechanism is based upon the observed coincidence between storm tracks and zonal asymmetry in the time-mean field, which does not always give us a consistent explanation.

The purpose of this study is to investigate the formation mechanism of the zonally localized storm tracks by using a version of T21-L20 CCSR/NIES AGCM (Numaguti et al., 1997). We perform three experiments under the perpetual January condition and analyze the data of 600 days after a spin-up period. The surface boundary conditions are idealized as follows. In T-run, Aqua Planet condition with zonally varying sea surface temperature (SST) in the tropics is assumed and warm water pool is located at 90°E (Fig. 1a). In E-run, Aqua Planet condition with zonally asymmetric SST gradient at 40°N is provided and sharp SST gradient is at 90°E (Fig. 1b). Finally in L-run, an idealized continent is placed in 90°E-90°W north to 20°N without mountains and SST is zonally uniform (Fig. 1c).

*Corresponding author address: Masaru Inatsu, Graduated school of Environmental Earth Science, Hokkaido University, Sapporo, Japan 060-0810; e-mail: inaz@ees.hokudai.ac.jp

2. RESULTS

We first focus on time-mean zonal wind in the upper troposphere. The time-mean zonal wind in L-run (Fig. 2c) is rather zonally uniform except for a weak intensification over the eastern edge of the continent. In E-run (Fig. 2b), it is perfectly zonally uniform. By contrast, in T-run (Fig. 2a), it has large zonal asymmetry with a maximum north to the tropical warm water pool at 90°E. The zonal variation in zonal wind speed exceeds 50 m s⁻¹. The importance of the tropical SST distribution on the formation of the subtropical jet core is clarified in Inatsu et al. (2000). Inatsu et al. (2001) discussed the formation mechanism of the westerly jet core by the tropical warm water pool. Corresponding to the horizontal distribution of subtropical westerlies, there are no robust stationary eddies in E-run (Fig. 3b), weak stationary eddies in higher latitudes in L-run (Fig. 3c), and robust subtropical stationary eddies in T-run (Fig. 3a).

We next investigate the relationship between storm tracks and time-mean westerly. In this study, the activity of transient eddies is measured by the root-mean-square high-pass filtered (<10 days; Blackmon, 1976) eddy kinetic energy. In T-run (Fig. 4a), the storm activity has a maximum downstream of the westerly jet core. In E-run (Fig. 4b), in spite of zonally uniform subtropical westerlies, the storm activity (Fig. 3b) is localized just over the sharp SST gradient. This suggests that large meridional SST gradient in the extratropics is important for localization of the storm tracks (*e.g.* Peng and Whitaker, 1999). Thus, the zonal variations in the westerly wind speed and stationary eddies in the upper troposphere are not necessarily related to localized storm tracks.

The relationship between upper-level storm tracks and lower-level baroclinicity is also examined. Here baroclinicity is defined as $0.31f|\partial\mathbf{u}/\partial z|/\mathcal{N}$ (Lindzen and Farrel, 1980), where $\mathbf{u} = (u, v)$ horizontal wind, f Coriolis parameter, and \mathcal{N} buoyancy frequency. In E-run (Fig. 5b), the extratropical SST gradient produces a rather zonal asymmetric baroclinicity, and the storm track is localized just over the sharp SST gradient (Fig. 4b). In L-run (Fig. 5c), the high baroclinicity region prevails over the ocean, but the storm track (Fig. 4c) exists even in low baroclinicity region over the land. By contrast, in T-run (Fig. 5a), storm tracks is

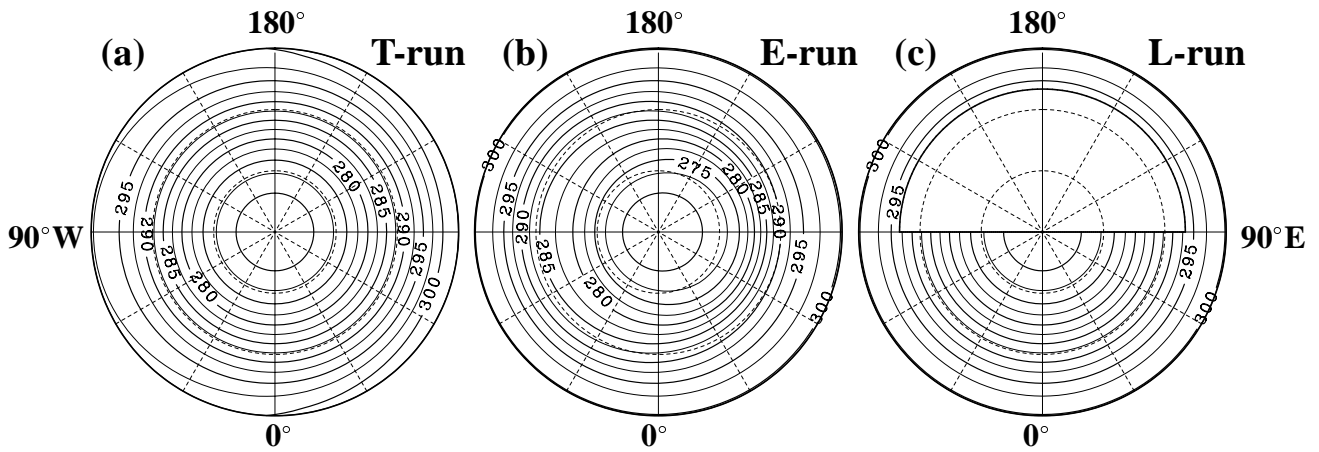


Figure 1: SST distribution for T- (a), E- (b), and L- (c) run. Contours interval is 2.5K. In L-run, the region of 90°E-90°W north to 20°N is the continent without mountains.

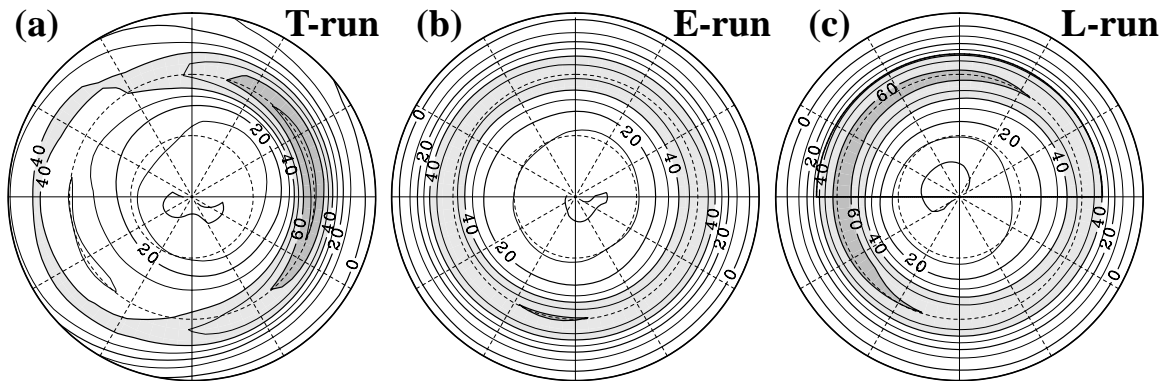


Figure 2: 250hPa Time-mean zonal wind in T- (a), E- (b), and L- (c) run. Contour intervals are 10 m s⁻¹. Light (heavy) shade indicates >40 (60) m s⁻¹.

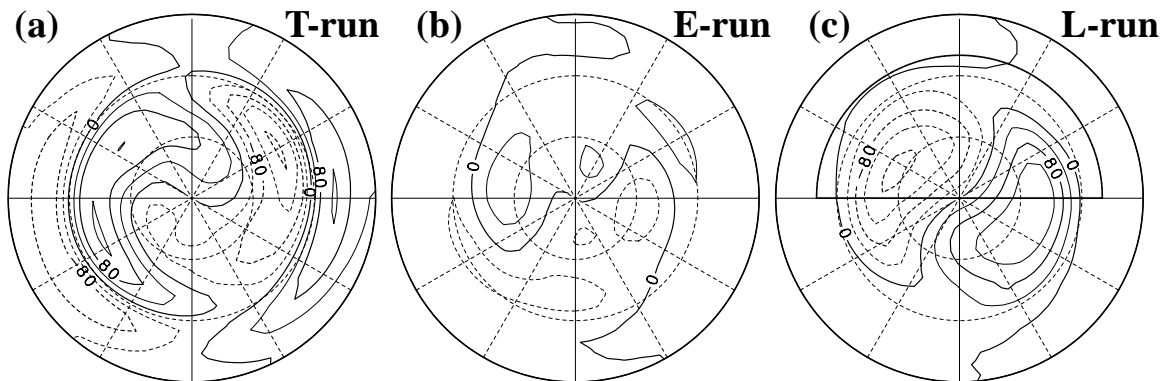


Figure 3: Same as Fig. 2, but for stationary eddy geopotential height. Contour intervals are 40 m and negative contours are dashed.

located downstream of the lower-level high baroclinicity region (Fig. 4a). Then the high baroclinicity in the lower atmosphere is not always accompanied with the

zonally localized storm tracks.

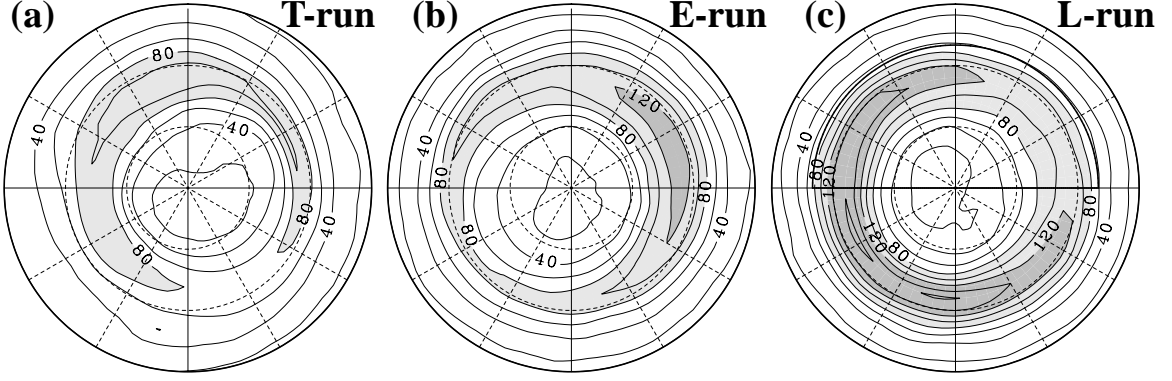


Figure 4: Same as Fig. 2, but for high-pass filtered eddy kinetic energy. Contour intervals are $20 \text{ m}^2 \text{ s}^{-2}$ and light and heavy shades indicate >80 and $>120 \text{ m}^2 \text{ s}^{-2}$, respectively.

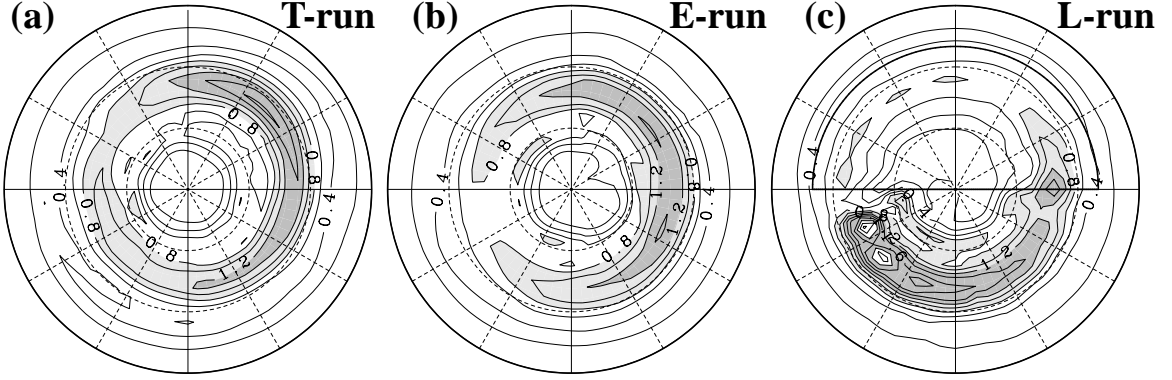


Figure 5: Same as Fig. 2, but for 900 hPa baroclinicity. Contour intervals are 0.2 day^{-1} and light and heavy shades indicate >0.8 and $>1.2 \text{ day}^{-1}$, respectively.

3. ENERGETICS

The eddy kinetic energy budget is analyzed for each experiment to examine the localization mechanism of storm tracks. The primitive equation is given as,

$$\frac{\partial \mathbf{u}}{\partial t} + (\mathbf{u} \cdot \nabla) \mathbf{u} + f \mathbf{k} \times \mathbf{u} = -\nabla \Phi, \quad (1)$$

where Φ is the geopotential height and \mathbf{k} the vertical unit vector. By decomposing the variables into the time-mean component (overbar) and the high-frequency (<10 days) eddies (prime) in Eq. (1), we obtain the kinetic energy equation of high-frequency eddies,

$$\left(\frac{\partial}{\partial t} + \bar{\mathbf{u}} \cdot \nabla \right) \mathcal{K}_E = C_F + C_C + C_T + \text{NL} + F, \quad (2)$$

where

$$\mathcal{K}_E = \frac{1}{2} (\overline{u'^2} + \overline{v'^2}),$$

$$\begin{aligned} C_F &= -\nabla \cdot \overline{\Phi' \mathbf{u}'}, \\ C_C &= -\frac{R}{p} \overline{\omega' T'} - \frac{\partial}{\partial p} \overline{\omega' \Phi'}, \\ C_T &= -\nabla \bar{\mathbf{u}} \cdot \overline{u' \mathbf{u}'} - \nabla \bar{\mathbf{v}} \cdot \overline{v' \mathbf{u}'}, \\ \text{NL} &= -\overline{\{(\mathbf{u} - \bar{\mathbf{u}}) \cdot \nabla (\mathbf{u} - \bar{\mathbf{u}})\}' u'} \\ &\quad - \overline{\{(\mathbf{u} - \bar{\mathbf{u}}) \cdot \nabla (\mathbf{v} - \bar{\mathbf{v}})\}' v'}. \end{aligned}$$

Here T temperature, ω vertical velocity, p pressure, and R gas constant. The first term in Eq. (2) is the advection of eddy kinetic energy, C_F the ageostrophic eddy energy flux divergence, C_C and C_T baroclinic and barotropic energy conversion, respectively, and NL the nonlinear effect, and F the mechanical damping (*e.g.* Chang and Orlanski, 1993).

We assess the magnitude of each term in Eq. (2) by integrating vertically from 150hPa to 850hPa. Figure 6 displays baroclinic and barotropic energy conversions and ageostrophic energy flux divergence in T-

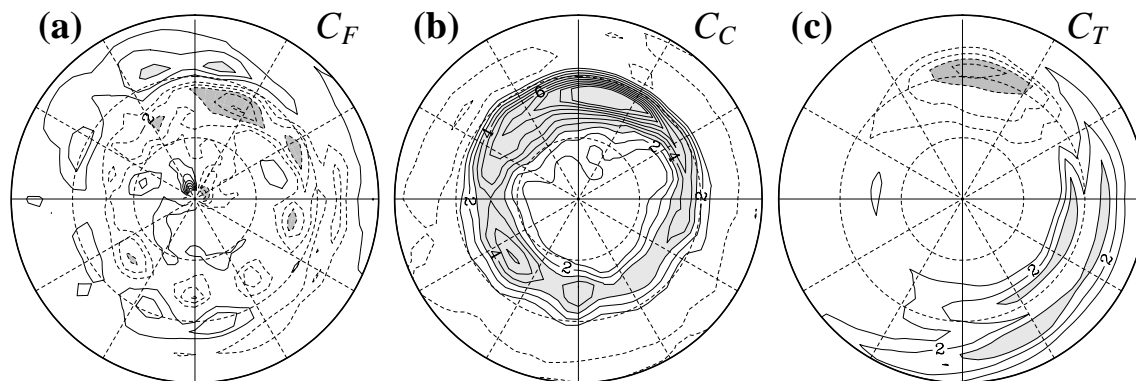


Figure 6: Energy budget for T-run. (a) ageostrophic eddy energy transfer (C_F), (b) baroclinic energy conversion (C_C) and (c) barotropic energy conversion (C_T). Contour intervals are $1 \text{ J m}^{-2} \text{ s}^{-1}$. Zero contours are omitted. Light (heavy) shade denotes >3 (< -3) $\text{J m}^{-2} \text{ s}^{-1}$. In positive (negative) regions, the eddies gain (lose) energy from (to) the mean flow.

run. The baroclinic energy conversion is positive just at the upper-level storm track region. The ageostrophic energy flux diverges downstream of the storm tracks, while it converges south of the storm track regions (near 20°N). This implies that the storm tracks could be zonally localized by diffusing the eddy activity to the equatorward due to the associated ageostrophic energy flux. Barotropic energy conversion is rather small compared with three two terms.

4. SUMMARY

Our idealized AGCM experiments suggest that the localization of storm tracks is not always associated with the westerly jet core and the lower-level high baroclinicity. The energy budget analysis shows that baroclinic energy conversion from the time-mean flow to the eddies coincides with the storm track regions and equatorward ageostrophic eddy energy flux is located at the downstream of the storm track.

REFERENCES

- Blackmon, M. L., 1976: A climatological spectral study of the 500mb geopotential height of the Northern Hemisphere. *J. Atmos. Sci.*, **33**, 1607-1623.
- , 1977: An observational study of the Northern Hemisphere wintertime circulation. *J. Atmos. Sci.*, **34**, 1040-1053.
- Chang, E. K. M., and I. Orlanski, 1993: On the dynamics of a storm track. *J. Atmos. Sci.*, **50**, 999-1015.
- Hoskins, B. J., and P. J. Valdes, 1990: On the existence of storm-tracks. *J. Atmos. Sci.*, **47**, 1854-1864.
- Inatsu, M., H. Mukougawa, and S.-P. Xie, 2000: Formation of subtropical westerly jet core in an idealized AGCM without mountains. *Geophys. Res. Lett.*, **29**, 529-532.
- , —, and —, 2001: Stationary eddy response to surface boundary forcing: Idealized GCM experiments, *J. Atmos. Sci.*, submitted.
- Lindzen, R. S., and B. Farrell, 1980: A simple approximate result for the maximum growth rate of baroclinic instabilities. *J. Atmos. Sci.*, **37**, 1648-1654.
- Numaguti, A., M. Takahashi, T. Nakajima, and A. Sumi, 1997: Description of CCSR/NIES atmospheric general circulation model. *CGER Super-computer Monograph Report*, **3**, 1-48. National Institute for Environmental Studies, Tukuba, Japan.
- Peng, S., and J. S. Whitaker, 1999: Mechanisms determining the atmospheric response to midlatitude SST anomalies. *J. Climate*, **12**, 1393-1408.
- Shutts, G. J., 1983: The propagation of eddies in diffluent jetstreams: eddy vorticity forcing of "blocking" flow fields. *Quart. J. Roy. Meteor. Soc.*, **109**, 737-761.
- Whitaker, J. S., and R. M. Dole, 1995: Organization of storm tracks in zonally varying flows. *J. Atmos. Sci.*, **52**, 1178-1190.